# A HIGH POWER PROTOTYPE OF A HARMONIC KICKER CAVITY

Gunn Tae Park, Gregory Grose, Jiquan Guo, Adam O'Brien, Sarah Overstreet, Robert Rimmer,
Scott Williams, and Haipeng Wang, Jefferson Lab, Newport News, VA 23606, USA

*Abstract*

In this paper, we report the progress on a harmonic kicker development as an injection device for the Rapid Cycling Synchrotron (RCS) of the Electron-Ion Collider (EIC). A harmonic kicker, a beam exchange device that can deflect the beam at an ultra-fast time scale (a few ns), has been developed in Jefferson Lab [1], [2]. The high power prototype that can deliver more than a 100 kV kick at 7 kW was recently fabricated and will be tested with a beam at Upgraded Injector Test Facility (UITF) in Jefferson Lab.

## INTRODUCTION

A harmonic kicker is a normal conducting RF device that delivers a deflecting kick on incoming bunches selectively over an ultra-fast time scale (~ ns). This becomes possible with an elaborate combination of five harmonic modes (see Fig. 1), which can be straightforwardly accommodated in a co-axial structure of the quarter wave resonator (QWR). Its first prototype was developed based on 95.2 MHz with a potential application as a beam exchange device to the Circulator Cooler Ring (CCR) of the Jefferson Lab Electron Ion Collider (JLEIC) [3].
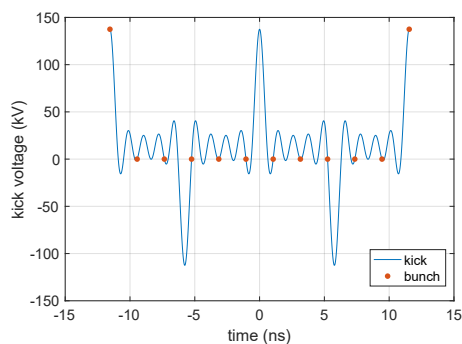


Figure 1: The temporal harmonic kick profile. The red dots correspond to the bunches at 476.3 MHz.

The upcoming second prototype (see Table 1 for the figures of merit), based on 86.6 MHz, is vacuum tight and prepared for the high power operation with the thermal analysis and cooling scheme applied, as well as for high current operation with its beam-coupling impedance checked [4]. This prototype can be beam-tested demonstrating its capability to selectively deflect the beam on MHz time scale. We plan the beam test at the UITF in Jefferson Lab. A successful test outcome would solidify the feasibility of the cavity as a beam injection device in the RCS of the EIC [5], [6], which is a recently found application of the kicker. In the RCS (as per a default 4-bunch scheme), a pair of a harmonic kickers—one with 147.8 MHz plus its third harmonic and the other with 2nd harmonic—can generate a sharp kick on injected bunches at a multiple of $f_{kick}$ = 73.9 MHz, while not affecting passing bunches at $f_{bunch}$ = 591 MHz (For more details, see [7]).

For a successful aforementioned operation, building and stably maintaining the designed kick profile (Fig. 1) in the real cavity is of critical importance. This is in turn achieved by the precise tuning of the frequencies, amplitudes, phases of all the harmonic modes. Thus during the fabrication of the cavity, special efforts were made to avoid geometry deformation on frequency-sensitive region of the cavity (for accurate frequency control), for precise insertion/alignment of tuning plungers (frequency) and power coupler antenna (for phase and amplitude via RF coupling $\beta$'s and also frequency) so that the deviation in those RF parameters during operation is well-within tolerance limit of the amplifier and control system (the LLRF and tuning system).

Table 1: The Figures of Merit for a Harmonic Kicker Cavity ($f$ : Freq. of Harmonic Modes, $R/Q_0$ : Shunt Resistance Over Quality Factor, $P_{wall}$ : Wall Loss, $\beta$ : RF Coupling Constant, $G$ : Geometry Factor, $V_k$ : Kick Voltage, The Numbers are for the High Power Operation as Originally Intended)

| Parameter | 1st | 2nd | 3rd | 4th | 5th |
|---|---|---|---|---|---|
| $f$ (MHz) | 86.6 | 259.8 | 433 | 606.2 | 779.4 |
| $R/Q_0$ ($\Omega$) | 241 | 76 | 41 | 25 | 14 |
| $P_{wall}$ (W) | 0.47 | 0.83 | 1.19 | 1.69 | 2.66 |
| $\beta$ | 0.74 | 1.21 | 1.22 | 1.20 | 1.25 |
| $G$ ($\Omega$) | 15 | 43 | 77 | 107 | 133 |
| $V_k$ (kV) | -25 | -25 | -25 | -25 | -25 |

## FABRICATION OF THE KICKER CAVITY

The kicker cavity parts were made of OFC (Oxygen free copper) and fabricated along two sub-assembly lines. One is an outer tube-line, where the parts were joined mostly by brazing, and the other is inner conductor-line, where the parts were machined and electron beam welded. In Figs. 2 and 3, two sub-assembely groups are shown. The outer tube group in Fig. 2 is made from 4 mm thick OFC tube with multiple ports brazed into. Brazing was done in a high vacuum furnace (see Fig. 2a) at 1035° (for 30 minutes) with a standard filler alloy 65Cu/35Ag. During the braze, the deformation of the cavity occurred despite the rounding clamps and other fixtures, around the port joints in particular. Consequently, the multiple repair brazes of the ports with the filler alloys at lower melting temperatures were inevitable (see Fig. 2b). The outer tube after going through many brazing cycles soft-

ened, vulnerable to further deformation. The inner conductor group in Fig. 3 was fabricated by CNC-machining (Fig. 3a) of the OFC tube and electron-beam welding (Fig. 3b).

As a final joint between the two subassemblies, "S-bond" low temperature brazing [8] replaced the EBW that was initially considered. The welding parameters were not giving a consistent performance on the full-penetration. Brazing also does not have a material shrinkage during the process, reducing uncertainty in the RF frequency shifts.
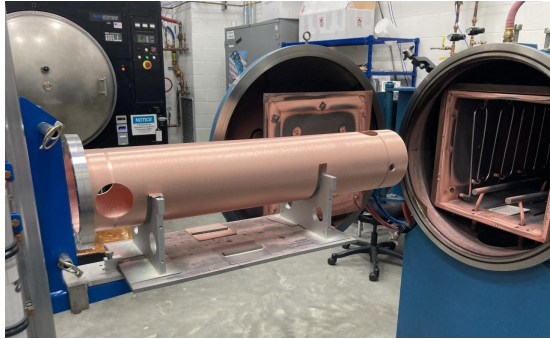


(a) The outer tube going into the braze furnace.



(b) The outer tube sub-assembly being leak-checked after the ports were brazed.

Figure 2: The outer tube sub-assembly.



(a) The center conductor CNC-machined for multiple tapering. (b) The center conductor sub-assembly in the welding chamber.

Figure 3: The center conductor sub-assembly.

## CLAMP-UP BENCH TEST

### Frequency Tuning Scheme

The nominal RF frequencies of the kicker cavity at its operation must be approached step by step because the fab-

rication and installation processes would involve inevitable frequency changes. Table 2 lists "the target frequency" that each procedure must achieve (after the procedure is done).

Table 2: The Target Frequency Table as Obtained from the Simulation (The Numbers Listed are in Unit of MHz After the Procedure)

| Procedure | Fab. complete | Evacuation | Operation |
|---|---|---|---|
| 1st | 86.588 | 86.613 | 86.6 |
| 2nd | 259.774 | 259.850 | 259.8 |
| 3rd | 432.956 | 433.081 | 433 |
| 4th | 606.138 | 606.313 | 606.2 |
| 5th | 779.319 | 779.543 | 779.4 |

In practice, the frequencies may have been shifted away from the target at the fabrication complete point, due to various fabrication errors. To access and compensate such frequency shifts, the fabricated sub-assemblies were assembled "clamped-up" before the final joint and the designated region of the cavity is trimmed away while tracking the frequencies. One can then obtain frequency response rate against trimming, which can be used to determine the final length of each part to reach the target frequency. The baseline trimming is a pair of cuts on both the outer and center conductors by the same amount. As shown in Fig. 4, the simulation predicts a linear fractional frequency response $\delta f/f \sim 1.2 \times 10^{-3}$/mm against the (baseline) trimming with all the slopes being (almost) identical. This implies that unlike a single frequency cavity case, the trimming of a harmonic kicker cavity can shift all the frequencies by the same fraction, but can not make the spread among the modes narrower. Thus the goal of the trimming is to bring the frequency (possibly the median deviation of the mode or the most power consuming mode, i.e., the 5th mode) to the target as close as possible, while leaving finer tuning for the rest of the modes to the tuner.
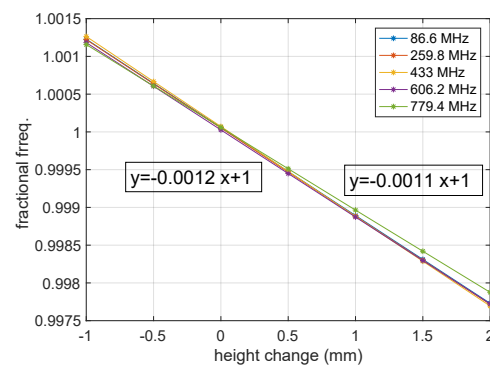


Figure 4: The fractional frequency response to trimming.

### Measurements & Analysis

The bench setup is shown in Fig. 5. The installation was done with great efforts for exact nominal insertions.

MC1: Circular and Linear Colliders

T12: Beam Injection/Extraction and Transport

Figure 5: The kicker cavity placed in the cage for the bench test. Its orientation is upside down for measurement convenience.

The frequency spectrum ($S_{12}$) for the five harmonic modes as it appears in the VNA measurement is shown in Fig. 6 and also listed in Table 3, which is in a good agreement with the prediction by the simulation except for the 5th mode, whose measurement heavily depended on the flange joint—to achieve nominal gap distance, the top-hat flange was "lifted up" by inserting the second gasket as a shim. The effects of field leakage through the gasket is the biggest on the 5th mode.
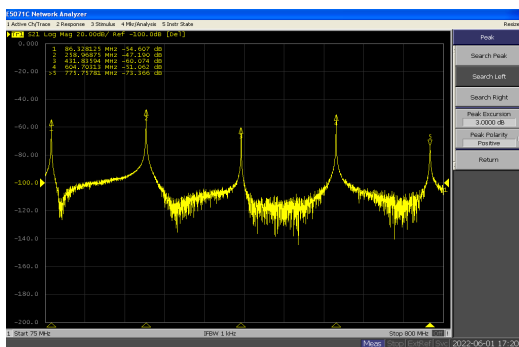


Figure 6: The harmonic mode spectrum on the VNA.

The RF coupling measurements was based on $S_{11}$ (linear scale) min/max (asymptotic) value, from which the coupling was obtained via approximate analytical formula.

The measurements/simulation are listed in Table 3. In particular, the 1st mode has a very good agreement with the simulated prediction. The other modes have poorer agreements. The possible explanation could be lower (unloaded) quality factor ($Q_0$) than expected due to a poor RF contacts among the clamped up parts, lower copper conductivity, and dirty RF surface. We expect the improvement on $Q_0$ after the final joint (by S-bonding) and chemical polishing. Also listed in Table 3 are frequency sensitivity of various inserted parts. The sensitivity of center conductor cap against shrink-

age (either by trimming or welding) was measured with the shims between the cap and the conductor tube. The sensitivity of the top-hat flange against insertion was measured using the shim between the flanges.

Table 3: The Various RF Measurements in Clamp-up Test (The Numbers Between Parenthesis are from Simulation and $\delta f$ is a Fractional Frequency Change)

| Mode | $f$ | $Q_L$ | $\beta$ | $\delta f / \Delta_{\mathrm{sh}}$ | $\delta f / \Delta_{\mathrm{bc}}$ |
|------|-----|-------|---------|------------------|------------------|
|      | MHz | -     | -       | $10^{-3}$/mm | $10^{-3}$/mm |
| 1st  | 86.410 | 3202 | 0.69 | -1.20 | -0.064 |
|      | (86.391) | (3276) | (0.74) | (-1.21) | (-0.066) |
| 2nd  | 259.050 | 5685 | 0.57 | -1.20 | -0.069 |
|      | (259.183) | (4434) | (1.21) | (-1.22) | (-0.071) |
| 3rd  | 431.900 | 10428 | 0.02 | -1.27 | -0.072 |
|      | (431.962) | (5766) | (1.22) | (-1.24) | (-0.078) |
| 4th  | 604.610 | 7776 | 0.2 | -1.26 | -0.049 |
|      | (604.770) | (6863) | (1.20) | (-1.27) | (-0.096) |
| 5th  | 778.186 | 2065 | 0.33 | -1.00 | -0.556 |
|      | (777.594) | (7333) | (1.25) | (-1.29) | (-0.130) |

Finally, the tuning matrix elements for a tuner were measured by receding the plungers with additional gasket in between the flanges and given in eq.(1). The matrix elements $\mathcal{T}_{ij}(i, j = 1, 2, \cdots, 5)$ in eq.(1) correspond to the frequency change (in MHz) of the $i$th mode against the $j$th plunger insertion by 1 mm. In comparison with the simulated prediction (the numbers between parenthesis), the elements involving lower order modes are almost identical with each other, while those involving higher order modes have some small discrepancy. This close agreement would lead to (fractional) frequency tuning range of $5 \times 10^{-4}$ (for all five modes), as predicted by the simulation.

$$\mathcal{T} = \begin{bmatrix} -0.018 & -0.010 & -0.002 & 0.009 & 0.014 \\ (-0.019) & (-0.012) & (-0.003) & (0.008) & (0.011) \\ 0.007 & 0.023 & -0.039 & -0.026 & 0.030 \\ (0.005) & (0.025) & (-0.043) & (-0.034) & (0.021) \\ 0.054 & -0.103 & 0.035 & -0.108 & -0.002 \\ (0.047) & (-0.114) & (0.032) & (-0.116) & (0.003) \\ -0.056 & 0.037 & -0.127 & -0.046 & -0.039 \\ (-0.068) & (0.035) & (-0.159) & (-0.094) & (-0.045) \\ -0.208 & -0.097 & 0.027 & -0.007 & -0.164 \\ (-0.226) & (-0.099) & (0.076) & (0.029) & (-0.121) \end{bmatrix}$$
(1)

## REFERENCES

[1] G.-T. Park, F. Fors, J. Guo, R. A. Rimmer, H. Wang, and S. Wang, "The Development of a New Fast Harmonic Kicker for the JLEIC Circulator Cooling Ring", in *Proc. IPAC'18*, Vancouver, Canada, Apr.-May 2018, pp. 1171–1173. doi:10.18429/JACoW-IPAC2018-TUPAL068

[2] G.-T. Park *et al.*, "Status Update of a Harmonic Kicker Development for JLEIC", in *Proc. IPAC'19*, Melbourne,

Australia, May 2019, pp. 3047–3050. `doi:10.18429/JACoW-IPAC2019-WEPRB099`

[3] Y. Huang, H. Wang, R. A. Rimmer, S. Wang, and J. Guo, "Ultrafast harmonic rf kicker design and beam dynamics analysis for an energy recovery linac based electron circulator cooler ring", *Phys. Rev. Accel. Beams*, vol. 19, p. 084201, 2016. `doi:10.1103/PhysRevAccelBeams.19.084201`

[4] G. Park, J. Guo, S. Wang, R. Rimmer, F. Marhauser, and H. Wang, "Beam impedance study on a harmonic kicker for the CCR of JLEIC", in *Proc. the 63rd ICFA Advanced Beam Dynamics Workshop on Energy Recovery Linacs*, Berlin, Germany, 2019.

[5] Brookhaven National Lab, "Electron-Ion Collider Conceptual Design Report", `https://www.bnl.gov/ec/`.

[6] N. Tsoupas *et al.*, "Beam Optics of the injection/extraction and beam transfer in the electron rings of the EIC project", presented at the IPAC'22, Bangkok, Thailand, Jun. 2022, paper WEPOPT047, this conference.

[7] G.-T. Park *et al.*, "RF Harmonic Kicker R&D Demonstration and Its Application to the RCS Injection of the EIC", in *Proc. IPAC'21*, Campinas, Brazil, May 2021, pp. 2632–2635. `doi:10.18429/JACoW-IPAC2021-WEPAB019`

[8] `https://s-bond.com`